Applied and Environmental Microbiology, Jan. 2011, p. 564–571 Vol. 77, No. 2
0099-2240/11/$12.00 doi:10.1128/AEM.01392-10

Influence of External Resistance on Electrogenesis, Methanogenesis, and Anode Prokaryotic Communities in Microbial Fuel Cells[▽]

Sokhee Jung and John M. Regan*

Department of Civil and Environmental Engineering, The Pennsylvania State University, University Park, Pennsylvania 16802

Received 10 June 2010/Accepted 3 November 2010

The external resistance (R_{ext}) of microbial fuel cells (MFCs) regulates both the anode availability as an electron acceptor and the electron flux through the circuit. We evaluated the effects of R_{ext} on MFCs using acetate or glucose. The average current densities (I) ranged from 40.5 mA/m^2 (9,800 Ω) to 284.5 mA/m^2 (150 Ω) for acetate-fed MFCs (acetate-fed reactors [ARs]), with a corresponding anode potential (E_{an}) range of −188 to −4 mV (versus a standard hydrogen electrode [SHE]). For glucose-fed MFCs (glucose-fed reactors [GRs]), I ranged from 40.0 mA/m^2 (9,800 Ω) to 273.0 mA/m^2 (150 Ω), with a corresponding E_{an} range of −189 to −7 mV. ARs produced higher Coulombic efficiencies and energy efficiencies than GRs over all tested R_{ext} levels because of electron and potential losses from glucose fermentation. Biogas production accounted for 14 to 18% of electron flux in GRs but only 0 to 6% of that in ARs. GRs produced similar levels of methane, regardless of the R_{ext}. However, total methane production in ARs increased as R_{ext} increased, suggesting that E_{an} might influence the competition for substrates between exoelectrogens and methanogens in ARs. An increase of R_{ext} to 9,800 Ω significantly changed the anode bacterial communities for both ARs and GRs, while operating at 970 Ω and 150 Ω had little effect. *Deltaproteobacteria* and *Bacteroidetes* were the major groups found in anode communities in ARs and GRs. *Betaproteobacteria* and *Gammaproteobacteria* were found only in ARs. *Bacilli* were abundant only in GRs. The anode-methanogenic communities were dominated by *Methanosaetaceae*, with significantly lower numbers of *Methanomicrobiales*. These results show that R_{ext} affects not only the E_{an} and current generation but also the anode biofilm community and methanogenesis.

The bioanode, a crucial component in bioelectrochemical systems (BESs), is composed of an anode biofilm and a conductive electrode. The main catalytic components of interest in anode biofilms are exoelectrogens, microorganisms that are capable of exocellular electron transfer (31). In mixed-culture systems, exoelectrogens compete for electron donors with other functional groups such as fermenters, acetogens, and methanogens. The complexity of anode biofilms makes it hard to elucidate electrochemical mechanisms at the bioanode, but a precise understanding of exoelectrogenesis and competition in anode biofilms will aid in improving the performance of BESs. Several reviews provide insightful summaries and perspectives regarding bioanodes (31, 34, 40, 43, 51).

The anode potential (E_{an}) is defined as the potential difference between the anode and the surrounding electrolyte (14). E_{an} also refers to the electromotive force that drives electrons to flow into an anode, and it is regarded as a measure of electron affinity (14). E_{an} is affected by intrinsic factors such as electrode material, electrolyte composition, electrochemical reactions, and catalysts (anode biofilm in BESs) (14). E_{an} also can be controlled extrinsically using a potentiostat or external resistances (R_{ext}). Potentiostats polarize the anode by varying the electrical energy input, while external resistances simply regulate E_{an} and the current without energy input. For example, the application of a low external resistance allows a relatively high E_{an} and current when the anode is connected to a highly oxidizing cathode.

There are conflicting results about the influence of E_{an} on start-up and sustained performance in BESs. Application of a high E_{an} (+200 mV versus Ag/AgCl) shortened the start-up of electrogenesis compared with the E_{an} of −360 mV (56). In another study, E_{an} did not affect the start-up time due to the use of an exoelectrogenic inoculum from another BES (1). At the start of this study, an anode poised at −200 mV versus Ag/AgCl had the highest maximum power density among systems poised at 0, −200, and −400 mV, but the performance of these systems converged by the end of the 1-month study. E_{an} was demonstrated to influence anode biofilm communities in microbial electrolysis cells (MECs) (52). A high E_{an} (370 mV versus standard hydrogen electrode [SHE]) created highly diverse and thin anode biofilms, with low current density and a low proportion of *Geobacteraceae*-like cells, while lower E_{an} values (−150, −90, and 20 mV) preferentially selected *Geobacteraceae*-like cells and produced high current density and thick biofilms (53). It was recently suggested that R_{ext} cannot be a valid tool for the improvement of anode biofilm performance because similar levels of maximum power were produced from potentially different anode biofilm communities enriched at different R_{ext} (32). However, this study did not provide electrochemical characterization to demonstrate whether the system was anode limited, nor did it address whether changes in R_{ext} influenced electron losses to competing metabolisms. Another recent study of cellulose-fed microbial fuel cells (MFCs) showed that R_{ext} affected power densities, with the highest maximum power density observed for reactors with the lowest R_{ext} (46). While this study showed screening-level differences in 16S rRNA genes from anode

* Corresponding author. Mailing address: Department of Civil and Environmental Engineering, The Pennsylvania State University, University Park, PA 16802. Phone: (814) 865-9436. Fax: (814) 863-7304. E-mail: jregan@engr.psu.edu.

▽ Published ahead of print on 12 November 2010.

biofilm and planktonic communities, the effect of R_{ext} on specific microbial populations was not determined.

Methanogenesis in BESs has also been investigated in terms of E_{an}. Methane production in a glucose-fed MFC incorporating a ferricyanide catholyte was not affected by E_{an} values between −220 to 200 mV versus SHE (13). An acetate-fed batch test with these glucose-acclimated communities showed negligible production of methane at an R_{ext} of 20 Ω (E_{an} of >100 mV versus SHE), suggesting that acetoclastic methanogenesis was not significant in these MFCs. That may have been influenced by the high current not allowing acetate utilization by the slow-growing acetoclastic methanogens. Another study showed that a flowthrough system fed with acetate (5.4 kg chemical oxygen demand [COD]/m^3/day) had increasing methane production as the anode potential decreased in the anode potential range of -300 mV $< E_{an} < -100$ mV versus SHE (55). In an ethanol-fed MFC, hydrogenotrophic *Methanomicrobiales* was the only detected methanogen (38). In MEC systems, hydrogenotrophic methanogenesis has been proposed as the main methanogenic pathway due to hydrogen flux to the anode (7, 26).

Control of R_{ext} is a simple method for studying bioelectrochemistry and exoelectrogenic ecology in MFCs. Furthermore, it can be a promising operational tool for MFC-incorporating wastewater treatment processes, as it is a system element that can be variable after design. The purpose of this study was to evaluate how R_{ext} affects the anode microbial community, electricity production, methane production, and electron flow without energy input from potentiostats. To achieve this goal, triplicate anode biofilms were developed at the same R_{ext} in H-shaped MFCs using glucose or acetate. Variations among anode microbial communities in triplicate MFCs were small, and their compositions were stable after four batch cycles (18). Then, they were operated and monitored at different R_{ext}. H-shaped MFCs provided comparatively stable E_{an} values during most of the batch cycles, which maintained nearly constant pressure for each anode microbial community. Our results showed that R_{ext} affected anode microbial community evolution when E_{an} substantially decreased. We also showed for the first time that acetoclastic *Methanosaetaceae* made up the main methanogenic group in acetate-fed MFCs, and their methanogenesis rate was affected by E_{an}. R_{ext} was demonstrated as a potential tool for controlling electrogenesis, methanogenesis, and anode microbial community.

MATERIALS AND METHODS

MFC construction and operation. H-shaped MFCs (two chambers separated by a Nafion membrane) were constructed as previously described with 25.2 cm^2 of anode (carbon paper; E-TEK) and 13.0 cm^2 of cathode (carbon paper coated with 0.35 mg Pt/cm^2; E-TEK) (18). Anode chambers were inoculated with anaerobic sludge from a secondary digester at the Pennsylvania State University Wastewater Treatment Plant. Two sets of triplicate reactors, acetate-fed reactors (ARs) fed sodium acetate (Sigma-Aldrich, MO) and glucose-fed reactors (GRs) fed D-glucose (EM Science, NJ), were operated with an R_{ext} of 970 Ω for four batches (stages 0 to 3, ca. 65 days). Afterwards, an R_{ext} of 9,800, 970, or 150 Ω was correspondingly applied to AR1/GR1, AR2/GR2, and AR3/GR3 for an additional three batch cycles (stages 4 to 6). Acetate-fed control reactors (ACs) and glucose-fed control reactors (GCs) were operated in an open circuit for stages 0 to 3 and then in a closed circuit at 970 Ω for stages 4 to 6 (Table 1). Anode chambers were filled with 210 ml medium (50 mM phosphate-buffered glucose minimal [GM] medium with 200 mg COD/liter or 25 meq electrons [e^-]/liter) in an anaerobic glove box. At the start of stages 1 to 3, the anode bottles were cleaned during the medium change, but this was discontinued at the end of stage 3. Cathode chambers were refilled with phosphate buffer (50 mM, pH 7.0) in each cycle and continuously aerated. Reactors were operated at 30°C.

TABLE 1. MFC operation scheme depicting applied R_{ext}

MFC	R_{ext} (Ω) at indicated stages	
	1 to 3	4 to 6
AC	Open circuit	970
AR1	970	9,800
AR2	970	970
AR3	970	150
GC	Open circuit	970
GR1	970	9,800
GR2	970	970
GR3	970	150

Electrochemical measurements. Cell voltage was monitored using a multiple data acquisition system (Pico, United Kingdom). Cathode potential was intermittently measured with a Ag/AgCl reference electrode (MF-2079; BASi) located about 5 mm from the cathode electrode, and anode potential was calculated by subtracting cathode potential from cell voltage. Electrode potentials were converted into SHE values by adding 195 mV and are reported throughout versus SHE. The Coulombic efficiency (CE) and the energy efficiency (EE) were calculated as previously described (29). Ohmic resistances of abiotic MFCs filled with the anolytes and catholyte mentioned above were measured using a potentiostat (PC 4/750; Gamry Instrument Inc., PA), and internal resistances (R_{int}) were calculated from the slopes of polarization curves.

Chemical analyses. Liquid samples were filtered with a syringe filter (0.2-μm Supor membrane; Pall Life Science, NY), and the soluble COD was measured using the colorimetric method (catalog no. 21258-15; Hach Co.). Duplicate headspace gas samples (100 μl) were collected using a gas-tight syringe for gas composition analyses at the end of each batch (24). Methane, carbon dioxide, hydrogen, and nitrogen concentrations in the headspace were analyzed by a GC (model 8610; SRI Instruments, CA) equipped with a thermal conductivity detector and a stainless steel column (1.8 m by 1/8 in.) packed with Porapak Q (Alltech, Deerfield, IL).

DNA extraction and PCR. Anode electrode samples (2 cm^2) were sliced with sterilized scissors at the end of each batch in an anaerobic chamber for isolation of genomic DNA. DNA was extracted with the PowerSoil DNA isolation kit (Mo Bio, CA), according to the manufacturer's instructions. The V3 regions of 16S rRNA genes were amplified with 534r (5′-ATTACCGCGGCTGCTGG-3′) and 341f (5′-CCTACGGGAGGCAGCAG-3′), with a GC clamp (5′-CGCCCGGG GCGCGCCCCGGGCGGGGCGGGGGCACGGGGGG-3′) attached to the 5′ termini (36). PCR amplifications were performed in a 10-μl volume containing 1.75 μl of DNA, 0.25 μM each primer (IDT, Inc., IA), 0.4 mg/ml of bovine serum albumin (Promega, WI), and *Taq* PCR master mix (Qiagen, CA), giving final concentrations as follows: 0.5 U of *Taq* polymerase, 200 μM of each deoxynucleoside triphosphate, and 3.0 mM $MgCl_2$. An iCycler IQ thermocycler (Bio-Rad, CA) was used for the PCR with the following program: initial denaturation at 95°C for 10 min; 10 touchdown cycles of denaturation at 94°C for 1 min, annealing at 65 to 55°C for 1 min (decreasing 1°C each cycle), and extension at 72°C for 2 min; 25 standard cycles of denaturation at 94°C for 1 min, annealing at 55°C for 1 min, and extension at 72°C for 2 min; and a final extension at 72°C for 30 min. Archaeal 16S rRNA genes were amplified with primers Arch958r (5′-YCCGGCGTTGAMTCCAATT-3′) and A20f (5′-TTCCGGTTGATCCYG CCRG-3′) in the above-described PCR composition using a PCR program described elsewhere (10).

Community analysis. Denaturing gradient gel electrophoresis (DGGE) was performed using the DCode universal mutation detection system (Bio-Rad, CA) for bacterial community analysis. PCR amplicons (10 μl) mixed with a loading dye were loaded onto 8% (wt/vol) polyacrylamide gels containing a gradient of denaturant ranging from 30 to 60% (100% denaturant was 7 M urea and 40% formamide). DGGE was run in 0.5× TAE (Tris-acetate-EDTA) buffer at 25 V for 15 min and subsequently at 200 V for 6 h (60°C). DGGE gels were silver stained (44). DGGE bands were excised and transferred to 30 μl elution buffer (Qiagen, CA) and incubated overnight at 4°C. Eluted DNAs were purified by PCR-DGGE until a single band was obtained in the target region to remove comigrated DNA with other melting domains. Operational taxonomic units (OTUs) were defined based on the melting domain. Single bands were eluted as described above and purified using DNA Clean & Concentrator-5 (Zymo, CA),

TABLE 2. Electrochemical properties of MFCs and performances under different R_{ext} conditions

MFC	R_{ext} (Ω)	R_{ohm} (Ω)[a]	R_{int} (Ω)[b]	E_{an} (mV)[c]	E_{cat} (mV)[c]	I (mA/m^2)[d]	P (mW/m^2)[d]
AC[e]	∞			−274 ± 10		NA	NA
AR1	9,800	1,003	1,200 ± 28	−188 ± 5	328 ± 5	40.5 ± 0.6	20.9 ± 0.6
AR2	970	1,003	1,368 ± 16	−76 ± 3	160 ± 4	187.5 ± 0.9	44.3 ± 0.4
AR3	150	1,115	1,398 ± 43	−4 ± 3	52 ± 3	284.5 ± 5.6	15.8 ± 0.6
GC[e]	∞			−269 ± 9		NA	NA
GR1	9,800	1,179	1,449 ± 18	−189 ± 4	320 ± 4	40.0 ± 0.4	20.4 ± 0.4
GR2	970	1,195	1,666 ± 41	−70 ± 3	142 ± 4	168.1 ± 1.7	35.6 ± 0.7
GR3	150	1,122	1,445 ± 33	−7 ± 3	46 ± 3	273.0 ± 3.5	14.5 ± 0.4

[a] Ohmic resistance of abiotic MFCs, measured by a potentiostat at an open circuit.
[b] Internal resistance of MFCs, measured from polarization curves.
[c] Anode potential (E_{an}) and cathode potential (E_{cat}) in the voltage plateau. E (versus SHE) = 195 mV + E (versus Ag/AgCl); n = 8.
[d] Current/power density based on the cathode (13 cm^2) because the anode area was variable due to anode sampling after each batch. NA, not applicable.
[e] R_{ext} is infinity under an open circuit during stages 2 and 3.

followed by sequencing. Archaeal clone libraries were constructed as previously described (18, 37). DNAs were sequenced at the Penn State University Nucleic Acid Facility. The DGGE profiles were converted into a matrix based on the locations and intensities of DGGE bands, and Minitab15 (Minitab Inc., PA) was used for principal component analysis (PCA) to convert the matrix into a two-dimensional PCA plot.

qPCR. Quantification of *Geobacteraceae* was performed with the primer set *Geobacteraceae*-494f (5′-AGGAAGCACCGGCTAACTCC-3′) and Geo825r (5′-TACCCGCRACACCTAGT-3′) (16). *Methanosaetaceae* and *Methanomicrobiales* were quantified using primer set Mst702f (5′-TAATCCTYGARGGACC ACCA-3′) and Mst862r (5′-CCTACGGCACCRACMAC-3′) and primer set MMB282f (5′-ATCGRTACGGGTTGTGGG-3′) and MMB832r (5′-CACCTA ACGCRCATHGTTTAC-3′) (58), respectively. Quantitative PCR (qPCR) was done in 20-μl volumes containing 1 μl DNA, 0.25 μM each primer (IDT, Inc., IA), 0.4 mg/ml bovine serum albumin (Promega, WI), and *Taq* PCR master mix (Qiagen, CA). qPCR was done in an iCycler IQ thermocycler (Bio-Rad, CA) with the program used by Yu et al. (58). Standard curves were made using plasmids containing an insert sequence of each targeted group. Plasmid concentrations were determined with a NanoDrop 2000 (Thermo Scientific). Total cell numbers were estimated using 16S rRNA genomic operon numbers of 2 for *Geobacteraceae* (35), 2 for *Methanosaetaceae*, and 2.67 for *Methanomicrobiales* (27).

Nucleotide sequence accession numbers. Nucleotide sequences were deposited in the GenBank database (accession numbers HM193296 to HM193368).

RESULTS

Electrochemistry. Exoelectrogenic community evolution, system performance, and replicate reactor reproducibility at 970 Ω for batches 0 to 3 were reported elsewhere (18). Following the stable and reproducible performance that was observed after 2 months at identical R_{ext} values, the R_{ext} was increased in one of the triplicate reactors and decreased in another for acetate- and glucose-fed systems. Low R_{ext} allowed high current flow and elevated the E_{an} (Table 2). Average currents in the voltage plateau ranged from 40.5 mA/m^2 (9,800 Ω) to 284.5 mA/m^2 (150 Ω) for ARs, with a corresponding E_{an} range of −188 to −4 mV. For the GRs, currents ranged from 40.0 mA/m^2 (9,800 Ω) to 273.0 mA/m^2 (150 Ω), with a corresponding E_{an} range of −189 to −7 mV. Cathode potential was also affected by R_{ext}, ranging from ~50 to ~330 mV. Lower average internal resistances of ARs (1,322 ± 107 Ω) than those of GRs (1,520 ± 126 Ω) contributed to higher power from ARs.

Electron flow and energy recovery. In lower R_{ext} (higher E_{an}) systems, the total substrate consumption rate was higher due to increased rates of electrogenesis (Table 3). COD loss not accounted for in measured current, hydrogen, and methane production and estimated aerobic respiration increased with R_{ext}, reaching 74% (ACs) and 64% (GCs) in an open circuit (R_{ext} = ∞). Acetate consistently resulted in higher CEs and EEs than glucose because of potential losses from glucose fermentation (13, 18). Biogas production accounted for 14 to 18% of elec-

TABLE 3. Average headspace gas compositions and electron flux distributions before and after changing external resistances

MFC	Headspace gas composition (μmol) in stages:				Electron flux (μeq/day) in stages 5 and 6[g]			Electron distribution and energy efficiency (%) in stages 5 and 6[g]				
	2 and 3		5 and 6									
	CH_4	CO_2	CH_4	CO_2	Total	Electricity	Methane	CE[a]	Biogas[b]	Aerobic[c]	Undefined[d]	EE[e]
AC[f]	1 ± 2	0 ± 0	0 ± 1	58 ± 21	143 ± 17	0 ± 0	0 ± 0	0 ± 0	0 ± 0	26 ± 3	74 ± 3	0 ± 0
AR1	28 ± 6	59 ± 9	30 ± 17	25 ± 9	193 ± 58	43 ± 2	10 ± 1	25 ± 6	6 ± 1	21 ± 9	47 ± 5	11 ± 2
AR2	30 ± 8	63 ± 13	24 ± 0	62 ± 17	347 ± 20	207 ± 3	14 ± 0	67 ± 6	5 ± 1	12 ± 2	17 ± 4	14 ± 1
AR3	13 ± 3	57 ± 11	0 ± 0	88 ± 4	481 ± 4	327 ± 6	0 ± 0	76 ± 10	0 ± 0	9 ± 1	16 ± 4	4 ± 1
GC[f]	51 ± 6	0 ± 0	90 ± 13	49 ± 8	170 ± 5	0 ± 0	25 ± 2	0 ± 0	15 ± 1	21 ± 1	64 ± 1	0 ± 0
GR1	46 ± 28	73 ± 6	91 ± 22	25 ± 16	224 ± 105	45 ± 2	29 ± 1	23 ± 9	18 ± 8	19 ± 12	41 ± 6	8 ± 3
GR2	43 ± 67	67 ± 7	92 ± 9	50 ± 16	343 ± 31	191 ± 2	57 ± 1	56 ± 4	17 ± 0	10 ± 1	17 ± 3	9 ± 1
GR3	54 ± 42	42 ± 37	84 ± 7	64 ± 14	543 ± 23	297 ± 0	67 ± 1	62 ± 5	14 ± 1	7 ± 1	16 ± 4	2 ± 0

[a] CE, Coulombic efficiency.
[b] Biogas = methane and hydrogen.
[c] Aerobic oxidation calculated based on the oxygen transfer coefficient (1.45×10^{-4} cm/s) through the proton exchange membrane (Nafion) (22).
[d] Undefined electron sink = 1 − (CE + biogas + aerobic).
[e] EE, energy efficiency.
[f] Control reactors were changed from open to closed circuit after stage 3.
[g] For AC and GC, values were taken from stages 2 and 3 when they were operated in an open circuit (R_{ext} = ∞).

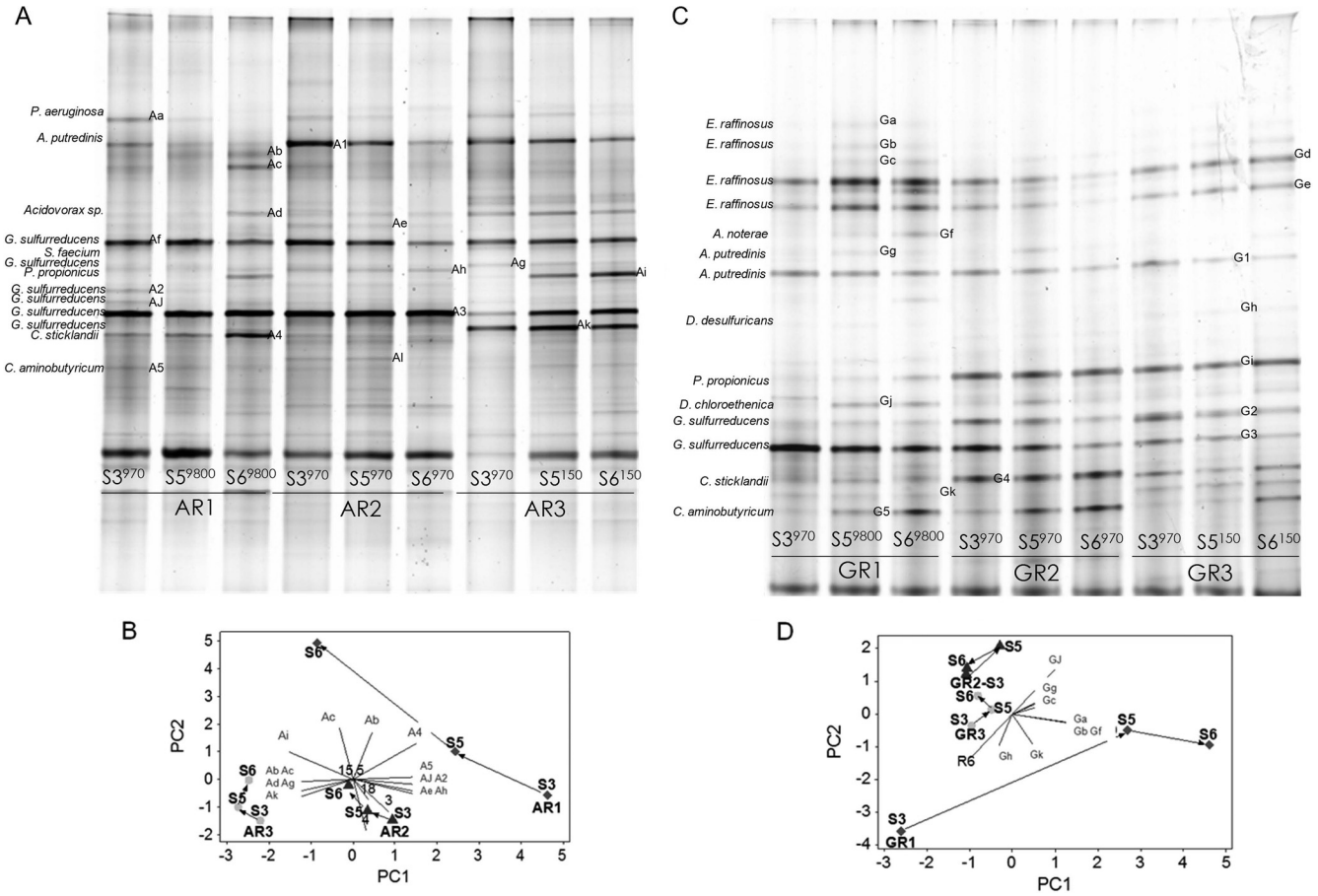

FIG. 1. Bacterial 16S rRNA gene-derived DGGE profiles (A and C) and their corresponding PCA plots (B and D), showing community evolution of anode biofilms in ARs (A and B) and GRs (C and D). S3 to S6, stages 3 to 6. Different external resistances were applied after stage 3. (Anode communities at stage 4 were not characterized.) *A. putredinis*, *Alistipes putredinis*; *S. faecium*, *Sphingobacterium faecium*; *E. raffinosus*, *Enterococcus raffinosus*; *A. noterae*, *Acetoanaerobium noterae*; *D. desulfuricans*, *Desulfovibrio desulfuricans*; *D. chloroethenica*, *Desulfuromonas chloroethenica*.

tron loss in GRs but only 0 to 6% of that in ARs. The high availability of the anode at low R_{ext} resulted in high CEs for both substrates. EEs were highest at 970 Ω (14% for AR2 and 9% for GR2), which was closest to the internal resistances of tested MFCs. Higher power density is earned when R_{ext} equals R_{int}, according to the following equation: $P = OCV^2 \{R_{ext}/[A(R_{ext} + R_{int})^2]\}$ (6), where P is the power density, OCV is the open-circuit voltage, and A is the electrode area.

Biogas production. Headspace biogas consisted mainly of methane and carbon dioxide, with negligible hydrogen detected. For acetate-fed reactors, total methane production increased as R_{ext} increased and the current decreased (Table 3). The nonwashing of anode chambers between batches did not affect methane production in ARs. Regardless of the current generation, ACs produced very little methane. GRs produced 43 to 54 μmol methane during stages 1 to 3 and 84 to 92 μmol in stages 5 and 6, during which the anode bottles were not washed with each medium change as they had been during stages 1 to 3 (Table 3). Regardless of the R_{ext}, GRs produced similar levels of methane, but cycle length-averaged methanogenesis rates varied significantly due to longer operation in higher R_{ext}. The nonelectrogenic GC produced an amount of methane similar to that of the closed-circuit GRs. The amount of produced carbon dioxide increased with decreasing R_{ext} and increasing current generation, and no carbon dioxide was detected in nonelectrogenic ACs and GCs.

***R*ext effect on anode prokaryotic communities.** Bacterial 16S rRNA genes were screened by DGGE and identified by band sequence analysis to determine the R_{ext} effect on the anode community composition and evolution (Fig. 1 and Table 4). Anode bacterial communities enriched at 970 Ω for four batches were compared with those that developed after the R_{ext} changes. Densitometry-based PCA showed that R_{ext} increasing to 9,800 Ω for both acetate- and glucose-fed MFCs changed the anode bacterial communities significantly, while continued operation at 970 Ω and a reduction to 150 Ω had little effect on them. The principal components for the community evolution observed in the 9,800-Ω systems were OTUs Ac, Ad, and Ai for AR1 and OTUs Ga, Gg, and GJ for GR1. OTUs G1, G2, G3, G4, and G5 of glucose-fed anode communities had nearly identical sequences and shared the same melting domains in DGGE correspondingly with OTUs A1, A2, A3, A4, and A5 of acetate-fed communities. *Deltaproteobacteria* and *Bacteroidetes* were the major taxonomic groups

TABLE 4. Phylogenetic identification of prominent DGGE bands

Band	GenBank closest isolate or enrichment-derived sequence (accession no.)	Class[a]	Identity (%)
A1/G1	*Alistipes putredinis* (AJ518876)	*Bacteroidetes*	92
A2/G2	*G. sulfurreducens* (AE017180)	*Deltaproteobacteria*	98
A3/G3	*G. sulfurreducens* (AE017180)	*Deltaproteobacteria*	99
A4/G4	*C. sticklandii* (M26494)	*Clostridia*	100
A5/G5	*C. aminobutyricum* (X76161)	*Clostridia*	99
Aa	*P. aeruginosa* (EF650089)	*Gammaproteobacteria*	100
Ac	Bacterial enrichment (FJ802369)	NA	93
Ad	*Acidovorax* sp. strain Ic3 (DQ421392)	*Betaproteobacteria*	100
Ae	Bacterial enrichment (EU082059)	NA	93
Af	*G. sulfurreducens* (AE017180)	*Deltaproteobacteria*	96
Ag	*Sphingobacterium faecium* (NR_025537)	*Sphingobacteria*	88
Ah	*G. sulfurreducens* (AE017180)	*Deltaproteobacteria*	96
Ai	*P. propionicus* (CP000482)	*Deltaproteobacteria*	96
AJ	*G. sulfurreducens* (AE017180)	*Deltaproteobacteria*	98
Ak	*G. sulfurreducens* (AE017180)	*Deltaproteobacteria*	95
Ga	*Enterococcus raffinosus* (FN600541)	*Bacilli*	99
Gb	*Enterococcus raffinosus* (FN600541)	*Bacilli*	100
Gd	*Enterococcus raffinosus* (FN600541)	*Bacilli*	99
Ge	*Enterococcus raffinosus* (FN600541)	*Bacilli*	99
Gg	*Alistipes putredinis* (AJ518876)	*Bacteroidetes*	93
Gh	*Desulfovibrio desulfuricans* (FJ655841)	*Deltaproteobacteria*	97
Gi	*P. propionicus* (CP000482)	*Deltaproteobacteria*	96
GJ	*Desulfuromonas chloroethenica* (NR_026012)	*Deltaproteobacteria*	91

[a] NA, not applicable.

commonly found in the anode communities of ARs and GRs. *Clostridia* was also a common group found in ARs and GRs. *Betaproteobacteria* (*Acidovorax* species) and *Gammaproteobacteria* (*Pseudomonas* species) were found only in ARs, and *Bacilli* (*Enterococcus* species) were abundantly detected only in GRs. In order to identify targets for quantifying methanogenic communities, clone libraries of archaeal 16S rRNA genes were constructed. The methanogenic communities in our anode biofilms were dominated by *Methanosaetaceae*. Most of the retrieved clones (40 out of 42) had the closest match to *Methanosaeta concilii* Opfikon (GenBank accession number NR_028242), with >99% similarity. The other two clones were affiliated with uncultured hydrogenotrophic *Methanomicrobiales* (19).

Quantification of three functional groups in anode biofilms. qPCR was used to quantify the cell number changes of three major functional groups (*Geobacteraceae*, *Methanosaetaceae*, and *Methanomicrobiales*) in the anode biofilms. In general, the R_{ext} change did not consistently affect the abundances of these functional groups (Fig. 2), though these data do not reveal their relative abundances in the total anode communities. The average cell numbers of *Geobacteraceae* were $1.7 \times 10^6 \pm 5.8 \times 10^5$ cells/cm^2 in ARs and $2.5 \times 10^6 \pm 1.6 \times 10^6$ cells/cm^2 in GRs. When ACs and GCs produced electricity, *Geobacteraceae* cell numbers increased drastically. The average *Methanosaetaceae* density was $2.0 \times 10^4 \pm 2.2 \times 10^4$ cells/cm^2 in ARs and $3.9 \times 10^4 \pm 1.9 \times 10^4$ cells/cm^2 in GRs. The average *Methanomicrobiales* density was $1.1 \times 10^3 \pm 2.1 \times 10^2$ cells/cm^2 in ARs. However, the average *Methanomicrobiales* density in GRs increased ca. 5 times from 2.0×10^3 cells/cm^2 in stage 3 to 1.2×10^4 cells/cm^2 in stage 6, with a doubling of methane production (Table 3). This coincided with the discontinuation of anode chamber washing between feedings, but nonwashing did not affect methane production or methanogen cell numbers in ARs. Regardless of the current generation, ACs produced very little methane and had only *Methanomicrobiales* cells. The nonelectrogenic GCs had less methanogenic cells in the anode biofilm but produced amounts of methane similar to those of the closed-circuit GRs.

Electricity production of open-circuit-acclimated anode biofilms. The open-circuit E_{an} values of ACs and GCs were initially ca. 50 mV, gradually decreasing to ca. −300 mV at the end of stage 1. In stage 1, acetate was barely consumed in ACs, while nearly all of the glucose added to GCs was converted to

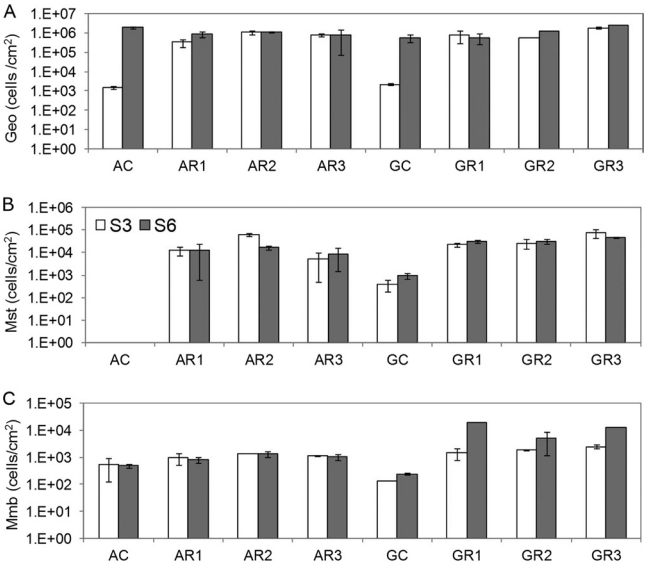

FIG. 2. Densities of *Geobacteraceae* (Geo), *Methanosaetaceae* (Mst), and *Methanomicrobiales* (Mmb) in anode biofilms at stage 3 (white) and stage 6 (gray), measured by quantitative PCR ($n = 2$).

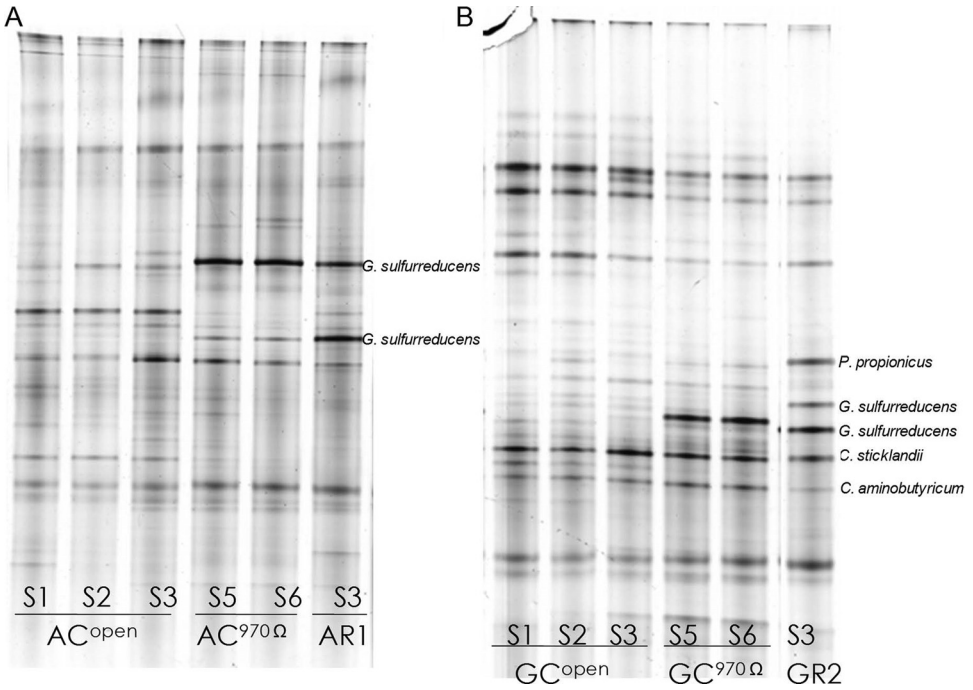

FIG. 3. Evolution of bacterial 16S rRNA gene-derived DGGE profiles from control reactor anode biofilms before and after electrogenesis. (A) Acetate-fed MFCs; (B) glucose-fed MFCs. S1 to S6, stages 1 to 6. Control reactors were changed from open to closed circuit after stage 3.

and accumulated as acetate. In successive batches, E_{an} remained ca. −300 mV, and metabolite concentrations fluctuated in both reactors. When circuits were connected with 970 Ω at stage 4, the current was generated immediately in both systems, and their E_{an} values rapidly increased to levels similar to those of AR2 and GR2. DGGE profiles of anode communities during stages 1 to 3 were similar and showed that *Geobacteraceae* sequences existed in the anode biofilms during open-circuit operation. Despite the unavailability of the anode for exoelectrogenic activity under the open-circuit condition, substantial substrate was consumed in these reactors during stages 2 and 3 (Table 3). Bands representing *Geobacteraceae* increased their intensities after circuit connection, which is consistent with the qPCR quantification, showing that the *Geobacteraceae* cell number increased ca. 10^3 times (Fig. 3). Anode biofilm profiles of electrogenic ACs and GCs had high similarities to those of AR1 and GR2, respectively.

DISCUSSION

External resistance effects on anode community evolution. Our results show that high R_{ext} affected the exoelectrogenic communities that had been established at 970 Ω. R_{ext} regulates E_{an}, which is equivalent to the anode availability as an electron acceptor. E_{an} influenced the competition between exoelectrogenic and nonexoelectrogenic community members, as supported by changes in the MFC performance with respect to electron distribution and biogas production (Table 3). E_{an} might also influence competition among exoelectrogens, either indirectly through microenvironmental conditions or directly through anode utilization, though we do not have direct evidence of this. For example, R_{ext} influences the substrate consumption rate (Table 3) and the associated proton production rate in the anode biofilm, so it can affect pH in the anode biofilm (12, 50). The anode biofilm community has been shown previously to be affected by pH in biohydrogenesis processes (44).

Regarding the direct effects of E_{an} on competition among exoelectrogenic populations, the lowest E_{an} (where the community changes were most pronounced) would select for exoelectrogens that can still meet their metabolic energy needs with such a small potential gradient between the redox potential of their electron donor and the anode. Most known *Geobacter* strains become significantly limited below potentials of about −0.15 V (45). Bacteria might adapt themselves to a specific potential by regulating intracellular reducing equivalents, such as the NADH/NAD^+ ratio, depending on the potential of the electron acceptor (30). For *Escherichia coli*, the NADH/NAD^+ ratio was 0.094 in aerobic growth and 0.22 in anaerobic growth (28) and increased progressively with decreasing midpoint potential of the electron acceptor (9). More fundamental bioelectrochemical studies are needed to address this redox issue.

Anode bacterial ecology. *Geobacter* strains appear to need a small amount of bicarbonate in the medium for crucial reactions, such as carbon fixation mediated by pyruvate-ferredoxin oxidoreductase (33). Accordingly, a low density of *Geobacter* cells in MFCs was thought to be associated with their poor growth in phosphate-buffered medium because high numbers of *Geobacter* 16S rRNA gene sequences were detected in carbonate-buffered anode chambers with scarce oxygen (4, 17). However, our result showing *Geobacter*-like cell dominance in phosphate-buffered MFCs with the headspace filled with nitrogen is coincident with previous results under the same con-

dition (18, 25, 57). It shows that the initial buffer species might not be an important factor in terms of *Geobacter* dominance in mixed-culture BESs, in which bicarbonate can be produced by other community members.

Desulfuromonas-like sequences were found in our GRs and were also detected in the anode community of an ethanol-fed MFC (23). *Desulfuromonas acetoxidans* is an acetate-utilizing electricity-producing species (2) and also oxidizes ethanol coupled with iron reduction (48). *Pelobacter*-like sequences detected in our systems were observed in sediment MFCs (15) and were predominant in ethanol-fed MECs (39). *Pelobacter propionicus*-like sequences were also abundant in an acetate-fed MEC system (5). *Acidovorax* sp. strain Ic3 is a hydrogenotrophic denitrifying bacterium (54), and similar sequences in acetate-fed anode biofilms (3, 57) and a cathode biofilm (42) were detected. These molecular evidences imply more research opportunities on potential electrogenesis of these genera. *Pseudomonas aeruginosa* produces electricity using electron shuttles (pyocyanin) (41), and related sequences in the anode biofilm of an acetate-fed MFC (57) were found, consistent with our results. *Enterococcus* is a genus of fermentative lactic acid bacteria, and an isolate of *Enterococcus gallinarum* exhibited oxidation and reduction peaks in cyclic voltammetry (21).

Bacteroidetes and *Clostridia* were common taxonomic groups in the anode biofilms of ARs and GRs. *Bacteroidetes* have been found in anode microbial communities of BESs fed starch-processing wastewater (20), cellulose (47), and acetate or glucose (57), but whether they contribute an exoelectrogenic phenotype in these communities is not known due to the absence of isolates from BESs. *Clostridium sticklandii* performs Stickland reactions, oxidizing an amino acid by reducing another amino acid (49). *Clostridium aminobutyricum* (GenBank accession number X76161; 99%) ferments 4-aminobutyrate to ammonia, acetate, and butyrate. Both species were also found in acetate- or glucose-fed single-chamber MFCs (57).

Methanogenic archaeal ecology. Methanogenesis was not affected by E_{an} in GRs. The nonwashing of anode chambers might have resulted in higher levels of methanogenesis during stages 5 and 6 in GRs, due to adhered microbial communities on the reactor walls that were not reflected in the qPCR data from anode electrodes. In ARs, the nonwashing of the anode chambers did not increase methanogenesis. Methanogenesis occurred only in MFCs harboring *Methanosaetaceae*-like sequences in their anode biofilms, suggesting that acetoclastic *Methanosaetaceae* can be the main methanogenic source in acetate-fed MFCs. As the E_{an} became higher, the current generation increased and methanogenesis diminished (Table 3). E_{an} might affect competition between exoelectrogens and acetoclastic methanogens in acetate-fed MFCs, with *Methanosaetaceae* being outcompeted in higher-current MFCs due to their lower affinity for and specific substrate utilization rate with acetate. For instance, pure culture *Geobacter sulfurreducens* has a half-saturation concentration (K_s) for acetate of 6.4 mg COD/liter (0.10 mM) and a specific substrate utilization rate (q_{max}) of 22.7 mg COD/mg volatile suspended solids (VSS) day^{-1} under ferric citrate-respiring conditions, while *Methanosaeta* spp. in methanogenic reactors have a K_s of 49 mg COD/liter and a q_{max} of 10.1 mg COD/mg VSS day^{-1} (8, 11). Thus, if anode availability is not limited, exoelectrogens could have a kinetic advantage over methanogens for acetate.

Not only acetoclastic *Methanosaetaceae* but also hydrogenotrophic *Methanomicrobiales* were detected in our systems. Hydrogenotrophic methanogenesis was suggested to be a main methanogenic pathway in MECs (7, 26). In an ethanol-fed MFC, *Methanomicrobiales* were the only methanogen (38); *Methanosaetaceae* might have been suppressed by the high concentration of substrate (initial COD of 2,500 mg/liter of ethanol) in this system due to their inhibition by high organic carbon concentrations (19). No *Methanosaetaceae* in the anode biofilms of ACs could be due to the initial oxic condition. During anode biofilm acclimation, the higher biomasses of the exoelectrogenic communities in closed-circuit ARs could create an ecological niche for *Methanosaetaceae* by consuming oxygen.

The differences between the internal resistances and ohmic resistances were 282 ± 84 Ω for ARs and 355 ± 104 Ω for GRs. Assuming that the overpotentials of abiotic cathodes were similar due to the high reproducibility of commercial cathode electrodes used in this experiment, the larger difference for GRs could be due to current-dependent anode overpotential, such as microbial activation, or metabolic loss, such as indirect glucose oxidation by mixed cultures (13, 18, 57) and higher diversity of anode biofilms in GRs. However, the high ohmic resistance of H-shaped MFCs precludes further electrochemical analysis on anode biofilm kinetics because power densities and current densities are limited by ohmic resistances in H-shaped MFCs, as shown previously (18). This ohmic limitation should be resolved by using BESs with low ohmic resistances.

ACKNOWLEDGMENTS

This research was supported by National Science Foundation grant CBET-0834033.

We thank Jungrae Kim (Sustainable Environment Research Center, United Kingdom) and Kion Kim (Department of Statistics, Penn State University) for their useful suggestions.

REFERENCES

1. **Aelterman, P., S. Freguia, J. Keller, W. Verstraete, and K. Rabaey.** 2008. The anode potential regulates bacterial activity in microbial fuel cells. Appl. Microbiol. Biotechnol. **78:**409–418.
2. **Bond, D. R., D. E. Holmes, L. M. Tender, and D. R. Lovley.** 2002. Electrode-reducing microorganisms that harvest energy from marine sediments. Science **295:**483–485.
3. **Borole, A. P., C. Y. Hamilton, T. Vishnivetskaya, D. Leak, and C. Andras.** 2009. Improving power production in acetate-fed microbial fuel cells via enrichment of exoelectrogenic organisms in flow-through systems. Biochem. Eng. J. **48:**71–80.
4. **Call, D. F., R. C. Wagner, and B. E. Logan.** 2009. Hydrogen production by *Geobacter* species and a mixed consortium in a microbial electrolysis cell. Appl. Environ. Microbiol. **75:**7579–7587.
5. **Chae, K.-J., M.-J. Choi, J. Lee, F. F. Ajayi, and I. S. Kim.** 2008. Biohydrogen production via biocatalyzed electrolysis in acetate-fed bioelectrochemical cells and microbial community analysis. Int. J. Hydrogen Energy **33:**5184–5192.
6. **Cheng, S., H. Liu, and B. E. Logan.** 2006. Increased power generation in a continuous flow MFC with advective flow through the porous anode and reduced electrode spacing. Environ. Sci. Technol. **40:**2426–2432.
7. **Clauwaert, P., and W. Verstraete.** 2009. Methanogenesis in membraneless microbial electrolysis cells. Appl. Microbiol. Biotechnol. **82:**829–836.
8. **Conklin, A., H. D. Stensel, and J. Ferguson.** 2006. Growth kinetics and competition between *Methanosarcina* and *Methanosaeta* in mesophilic anaerobic digestion. Water Environ. Res. **78:**486–496.
9. **de Graef, M. R., S. Alexeeva, J. L. Snoep, and M. J. Teixeira de Mattos.** 1999. The steady-state internal redox state (NADH/NAD) reflects the external redox state and is correlated with catabolic adaptation in Escherichia coli. J. Bacteriol. **181:**2351–2357.

10. **DeLong, E. F., L. T. Taylor, T. L. Marsh, and C. M. Preston.** 1999. Visualization and enumeration of marine planktonic archaea and bacteria by using polyribonucleotide probes and fluorescent in situ hybridization. Appl. Environ. Microbiol. **65:**5554–5563.
11. **Esteve-Nunez, A., M. Rothermich, M. Sharma, and D. Lovley.** 2005. Growth of *Geobacter sulfurreducens* under nutrient-limiting conditions in continuous culture. Environ. Microbiol. **7:**641–648.
12. **Franks, A. E., K. P. Nevin, H. Jia, M. Izallalen, T. L. Woodard, and D. R. Lovley.** 2009. Novel strategy for three-dimensional real-time imaging of microbial fuel cell communities: monitoring the inhibitory effects of proton accumulation within the anode biofilm. Energy Environ. Sci. **2:**113–119.
13. **Freguia, S., K. Rabaey, Z. G. Yuan, and J. Keller.** 2008. Syntrophic processes drive the conversion of glucose in microbial fuel cell anodes. Environ. Sci. Technol. **42:**7937–7943.
14. **Hamann, C., A. Hamnett, and W. Vielstich.** 2007. Electrochemistry, 2nd ed., p. 77. Wiley-VCH, Weinheim, NY.
15. **Holmes, D. E., D. R. Bond, R. A. O'Neil, C. E. Reimers, L. R. Tender, and D. R. Lovley.** 2004. Microbial communities associated with electrodes harvesting electricity from a variety of aquatic sediments. Microb. Ecol. **48:**178–190.
16. **Holmes, D. E., K. T. Finneran, R. A. O'Neil, and D. R. Lovley.** 2002. Enrichment of members of the family Geobacteraceae associated with stimulation of dissimilatory metal reduction in uranium-contaminated aquifer sediments. Appl. Environ. Microbiol. **68:**2300–2306.
17. **Ishii, S. I., K. Watanabe, S. Yabuki, B. E. Logan, and Y. Sekiguchi.** 2008. Comparison of electrode reduction activities of *Geobacter sulfurreducens* and an enriched consortium in an air-cathode microbial fuel cell. Appl. Environ. Microbiol. **74:**7348–7355.
18. **Jung, S., and J. M. Regan.** 2007. Comparison of anode bacterial communities and performance in microbial fuel cells with different electron donors. Appl. Microbiol. Biotechnol. **77:**393–402.
19. **Karakashev, D., D. J. Batstone, and I. Angelidaki.** 2005. Influence of environmental conditions on methanogenic compositions in anaerobic biogas reactors. Appl. Environ. Microbiol. **71:**331–338.
20. **Kim, B. H., H. S. Park, H. J. Kim, G. T. Kim, I. S. Chang, J. Lee, and N. T. Phung.** 2004. Enrichment of microbial community generating electricity using a fuel-cell-type electrochemical cell. Appl. Microbiol. Biotechnol. **63:**672–681.
21. **Kim, G. T., M. S. Hyun, I. S. Chang, H. J. Kim, H. S. Park, B. H. Kim, S. D. Kim, J. W. Wimpenny, and A. J. Weightman.** 2005. Dissimilatory Fe(III) reduction by an electrochemically active lactic acid bacterium phylogenetically related to *Enterococcus gallinarum* isolated from submerged soil. J. Appl. Microbiol. **99:**978–987.
22. **Kim, J. R., S. Cheng, S. E. Oh, and B. E. Logan.** 2007. Power generation using different cation, anion, and ultrafiltration membranes in microbial fuel cells. Environ. Sci. Technol. **41:**1004–1009.
23. **Kim, J. R., S. H. Jung, J. M. Regan, and B. E. Logan.** 2007. Electricity generation and microbial community analysis of alcohol powered microbial fuel cells. Bioresour. Technol. **98:**2568–2577.
24. **Kim, J. R., B. Min, and B. E. Logan.** 2005. Evaluation of procedures to acclimate a microbial fuel cell for electricity production. Appl. Microbiol. Biotechnol. **68:**23–30.
25. **Lee, H.-S., P. Parameswaran, A. Kato-Marcus, C. I. Torres, and B. E. Rittmann.** 2008. Evaluation of energy-conversion efficiencies in microbial fuel cells (MFCs) utilizing fermentable and non-fermentable substrates. Water Res. **42:**1501–1510.
26. **Lee, H.-S., C. S. I. Torres, P. Parameswaran, and B. E. Rittmann.** 2009. Fate of H2 in an upflow single-chamber microbial electrolysis cell using a metal-catalyst-free cathode. Environ. Sci. Technol. **43:**7971–7976.
27. **Lee, Z. M., C. Bussema III, and T. M. Schmidt.** 2009. rrnDB: documenting the number of rRNA and tRNA genes in bacteria and archaea. Nucleic Acids Res. **37:**D489–D493.
28. **Leonardo, M. R., Y. Dailly, and D. P. Clark.** 1996. Role of NAD in regulating the adhE gene of Escherichia coli. J. Bacteriol. **178:**6013–6018.
29. **Liu, H., S. Cheng, and B. E. Logan.** 2005. Production of electricity from acetate or butyrate using a single-chamber microbial fuel cell. Environ. Sci. Technol. **39:**658–662.
30. **Logan, B. E.** 2008. Microbial fuel cells. Wiley-Interscience, Hoboken, NJ.
31. **Logan, B. E., and J. M. Regan.** 2006. Electricity-producing bacterial communities in microbial fuel cells. Trends Microbiol. **14:**512–518.
32. **Lyon, D. Y., F. Buret, T. M. Vogel, and J.-M. Monier.** 2010. Is resistance futile? Changing external resistance does not improve microbial fuel cell performance. Bioelectrochemistry **78:**2–7.
33. **Mahadevan, R., D. R. Bond, J. E. Butler, A. Esteve-Nunez, M. V. Coppi, B. O. Palsson, C. H. Schilling, and D. R. Lovley.** 2006. Characterization of metabolism in the Fe(III)-reducing organism Geobacter sulfurreducens by constraint-based modeling. Appl. Environ. Microbiol. **72:**1558–1568.
34. **Marcus, A. K., C. I. Torres, and B. E. Rittmann.** 2007. Conduction-based modeling of the biofilm anode of a microbial fuel cell. Biotechnol. Bioeng. **98:**1171–1182.
35. **Methe, B. A., K. E. Nelson, J. A. Eisen, I. T. Paulsen, W. Nelson, J. F. Heidelberg, D. Wu, M. Wu, N. Ward, M. J. Beanan, R. J. Dodson, R. Madupu, L. M. Brinkac, S. C. Daugherty, R. T. DeBoy, A. S. Durkin, M. Gwinn, J. F. Kolonay, S. A. Sullivan, D. H. Haft, J. Selengut, T. M. Davidsen, N. Zafar, O. White, B. Tran, C. Romero, H. A. Forberger, J. Weidman, H. Khouri, T. V. Feldblyum, T. R. Utterback, S. E. Van Aken, D. R. Lovley, and C. M. Fraser.** 2003. Genome of *Geobacter sulfurreducens*: metal reduction in subsurface environments. Science **302:**1967–1969.
36. **Muyzer, G., T. Brinkhoff, U. Nubel, C. Santegoeds, H. Schafer, and C. Wawer.** 2004. Molecular microbial ecology manual, 2nd ed., p. 743–770. Kluwer Academic Publishers, Dordrecht, Netherlands.
37. **Nicol, G. W., D. Tscherko, T. M. Embley, and J. I. Prosser.** 2005. Primary succession of soil Crenarchaeota across a receding glacier foreland. Environ. Microbiol. **7:**337–347.
38. **Parameswaran, P., C. I. Torres, H.-S. Lee, R. Krajmalnik-Brown, and B. E. Rittmann.** 2009. Syntrophic interactions among anode respiring bacteria (ARB) and non-ARB in a biofilm anode: electron balances. Biotechnol. Bioeng. **103:**513–523.
39. **Parameswaran, P., H. Zhang, C. I. Torres, B. E. Rittmann, and R. Krajmalnik-Brown.** 2009. Microbial community structure in a biofilm anode fed with a fermentable substrate: the significance of hydrogen scavengers. Biotechnol. Bioeng. **105:**69–78.
40. **Pham, T. H., P. Aelterman, and W. Verstraete.** 2009. Bioanode performance in bioelectrochemical systems: recent improvements and prospects. Trends Biotechnol. **27:**168–178.
41. **Rabaey, K., N. Boon, M. Hofte, and W. Verstraete.** 2005. Microbial phenazine production enhances electron transfer in biofuel cells. Environ. Sci. Technol. **39:**3401–3408.
42. **Rabaey, K., S. T. Read, P. Clauwaert, S. Freguia, P. L. Bond, L. L. Blackall, and J. Keller.** 2008. Cathodic oxygen reduction catalyzed by bacteria in microbial fuel cells. ISME J. **2:**519–527.
43. **Rabaey, K., J. Rodriguez, L. L. Blackall, J. Keller, P. Gross, D. Batstone, W. Verstraete, and K. H. Nealson.** 2007. Microbial ecology meets electrochemistry: electricity-driven and driving communities. ISME J. **1:**9–18.
44. **Ren, N., D. Xing, B. E. Rittmann, L. Zhao, T. Xie, and X. Zhao.** 2007. Microbial community structure of ethanol type fermentation in bio-hydrogen production. Environ. Microbiol. **9:**1112–1125.
45. **Richter, H., K. P. Nevin, H. Jia, D. A. Lowy, D. R. Lovley, and L. M. Tender.** 2009. Cyclic voltammetry of biofilms of wild type and mutant Geobacter sulfurreducens on fuel cell anodes indicates possible roles of OmcB, OmcZ, type IV pili, and protons in extracellular electron transfer. Energy Environ. Sci. **2:**506–516.
46. **Rismani-Yazdi, H., A. D. Christy, S. M. Carver, Z. Yu, B. A. Dehority, and O. H. Tuovinen.** 2011. Effect of external resistance on bacterial diversity and metabolism in cellulose-fed microbial fuel cells. Bioresour. Technol. **102:**278–283.
47. **Rismani-Yazdi, H., A. D. Christy, B. A. Dehority, M. Morrison, Z. Yu, and O. H. Tuovinen.** 2007. Electricity generation from cellulose by rumen microorganisms in microbial fuel cells. Biotechnol. Bioeng. **97:**1398–1407.
48. **Roden, E. E., and D. R. Lovley.** 1993. Dissimilatory Fe(III) reduction by the marine microorganism *Desulfuromonas acetoxidans*. Appl. Environ. Microbiol. **59:**734–742.
49. **Stadtman, T. C., and L. S. McClung.** 1957. Clostridium sticklandii nov. spec. J. Bacteriol. **73:**218–219.
50. **Torres, C. I., A. Kato Marcus, and B. E. Rittmann.** 2008. Proton transport inside the biofilm limits electrical current generation by anode-respiring bacteria. Biotechnol. Bioeng. **100:**872–881.
51. **Torres, C. I., A. K. Marcus, H. S. Lee, P. Parameswaran, R. Krajmalnik-Brown, and B. E. Rittmann.** 2010. A kinetic perspective on extracellular electron transfer by anode-respiring bacteria. FEMS Microbiol. Rev. **34:**3–17.
52. **Torres, C. I., A. K. Marcus, P. Parameswaran, and B. E. Rittmann.** 2008. Kinetic experiments for evaluating the Nernst-Monod model for anode-respiring bacteria (ARB) in a biofilm anode. Environ. Sci. Technol. **42:**6593–6597.
53. **Torres, C. S. I., R. Krajmalnik-Brown, P. Parameswaran, A. K. Marcus, G. Wanger, Y. A. Gorby, and B. E. Rittmann.** 2009. Selecting anode-respiring bacteria based on anode potential: phylogenetic, electrochemical, and microscopic characterization. Environ. Sci. Technol. **43:**9519–9524.
54. **Vasiliadou, I. A., S. Siozios, I. T. Papadas, K. Bourtzis, S. Pavlou, and D. V. Vayenas.** 2006. Kinetics of pure cultures of hydrogen-oxidizing denitrifying bacteria and modeling of the interactions among them in mixed cultures. Biotechnol. Bioeng. **95:**513–525.
55. **Virdis, B., K. Rabaey, Z. Yuan, R. A. Rozendal, and J. R. Keller.** 2009. Electron fluxes in a microbial fuel cell performing carbon and nitrogen removal. Environ. Sci. Technol. **43:**5144.
56. **Wang, X., Y. Feng, N. Ren, H. Wang, H. Lee, N. Li, and Q. Zhao.** 2009. Accelerated start-up of two-chambered microbial fuel cells: effect of anodic positive poised potential. Electrochim. Acta **54:**1109–1114.
57. **Xing, D., S. Cheng, J. M. Regan, and B. E. Logan.** 2009. Change in microbial communities in acetate- and glucose-fed microbial fuel cells in the presence of light. Biosens. Bioelectron. **25:**105–111.
58. **Yu, Y., C. Lee, J. Kim, and S. Hwang.** 2005. Group-specific primer and probe sets to detect methanogenic communities using quantitative real-time polymerase chain reaction. Biotechnol. Bioeng. **89:**670–679.